HOLIGILM: Hollow light guide interior illumination method – An analytic calculation approach for cylindrical light-tubes

ARTICLE *in* SOLAR ENERGY · MARCH 2008

Impact Factor: 3.47 · DOI: 10.1016/j.solener.2007.07.003

3 AUTHORS, INCLUDING:

Stanislav Darula
Slovak Academy of Sciences
79 PUBLICATIONS **349** CITATIONS

SEE PROFILE

Richard Kittler
Slovak Academy of Sciences
75 PUBLICATIONS **500** CITATIONS

SEE PROFILE

Available online at www.sciencedirect.com
ScienceDirect
Solar Energy 82 (2008) 247–259
SOLAR ENERGY
www.elsevier.com/locate/solener

HOLIGILM: Hollow light guide interior illumination method – An analytic calculation approach for cylindrical light-tubes

M. Kocifaj *, S. Darula [1], R. Kittler

ICA, Slovak Academy of Sciences, 9, Dúbravská Road, 845 03 Bratislava, Slovak Republic

Received 4 April 2007; accepted 19 July 2007
Available online 15 August 2007

Communicated by: Associate Editor Jean-Louis Scartezzini

Abstract

A physical model for interior illuminance calculation HOLIGILM applied to cylindrical skylights was developed. Based on the ray-tracing between the diffuser of a tubular skylight and the sky vault including the Sun, the light transmission coefficient of the cover dome and of the interior diffuser with the high light-guide reflection, as well as taking into account the geometry of the interior, the resulting illuminance of the working plane can be analysed. As the model is strictly physical it allows to study influences of optical properties of tubular skylights (dome, tube and diffuser) on the interior daylight illuminance distribution specifying the luminance distribution on the hollow light-guide diffuser. The standard sky luminance distributions adopted ISO 15469:2004 and the new solar luminance and constant were included into the evaluation concept of tubular skylight. In addition to the original formulae some practical examples of the predicted illuminance on the working plane are also presented in this paper.

Keywords: Hollow light guides; Tubular skylight; Roof-light; Sky luminance; Interior illuminance

1. Introduction

Recently different hollow light guides were introduced to utilise daylight in those interiors where traditional windows for any reason cannot be used (Rosemann and Kaase, 2005), e.g. in extensive or underground spaces, deep staircases, etc. Vertical hollow light guides sometimes replace older light wells covered with white paint, but these are now specially manufactured tubes with internally high reflective surfaces. These metallic mirror light guides collect both skylight and sunlight flux falling on the horizontal upper opening and forward it downward by multiple inter-reflections onto the diffusing glazing at the bottom of the tube. This diffuser has to redistribute daylight in the interior space, i.e. on its working plane, floor or walls (Swift and Smith, 1995; Plch and Mohelnikova, 2005a; Plch and Mohelnikova, 2005b).

Any daylight available outdoors is specified by the luminance distribution on the sky vault plus the luminance of the Sun disk when it is not shaded by clouds. All effective luminance patches enter the light guide opening differently within their small solid angles and due to mirror reflections proceed down the tube as imagined beams. However, all daylight has to pass usually also through a transparent hemispherical dome covering the tube and every beam is reflected by differently oriented patches of the cylindrical tube surface. Thus theoretically a very complex task is to be solved involving:

- the specification of luminance distributions of the upper half-space facing the roof opening of the light guide,
- the flux transmission losses caused by the light-guide dome cover,

* Corresponding author. Tel.: +421 2 54775157; fax: +421 2 54773548.
E-mail address: kocifaj@savba.sk (M. Kocifaj).
[1] Member of ISES.

0038-092X/$ - see front matter © 2007 Elsevier Ltd. All rights reserved.
doi:10.1016/j.solener.2007.07.003

Nomenclature

a, b	parameters of the gradation function
a_v	luminous extinction coefficient for the ideally clear atmosphere
c, d, e	parameters of the indicatrix function
D	tube diameter (m)
D_v	horizontal diffuse sky illuminance (lx)
$E_{\mathrm{i,D}}$	illuminance of element on the diffuser (lx)
$E_{\mathrm{i,W}}$	illuminance of element on the interior working plane (lx)
E_v	horizontal extraterrestrial illuminance (lx)
E_{vo}	luminous solar constant (lx)
$f(Z_{\mathrm{S}})$	indicatrix function for solar zenith angle
$f(\chi)$	indicatrix function for sky element with angle χ from the Sun
G_v	horizontal global illuminance (lx)
H	height of the vertical cylindrical tube (m)
H/D	aspect ratio
$j(\vartheta, \phi, \phi_0, r_0)$	sky luminance reaching the diffuser transported by the tube
$j_{\mathrm{S}}(\vartheta, \phi, \phi_0, r_0)$	sun luminance reaching the diffuser transported by the tube
$j_{\mathrm{T}}(\vartheta, \phi, \phi_0, r_0)$	total, sky and sun luminance reaching the diffuser transported by the tube
k_i	coefficients of proportionality
L_{a}	luminance of the arbitrary sky element (cd/m^2)
L_{vo}	extraterrestrial luminance of the solar disk (kcd/m^2)
L_{S}	sun luminance seen at ground level (kcd/m^2)
L_{z}	zenith luminance (cd/m^2)
$L(\zeta, \alpha - \alpha_{\mathrm{S}})$	sky luminance (cd/m^2)
M	number of sun-beams reaching the same diffuser element from various directions
m	relative optical air mass of the atmosphere
N	number of reflections of a particular beam
N_{Sun}	number of sun beam reflections
$\mathbf{n}_1$	upward-directed unit vector from the surface element of the diffuser
$\mathbf{n}_2$	unit vector after first reflection (considering upward ray-tracing)
$\mathbf{n}_v$	unit vector normal to the surface of the cylinder in any point of reflection
$\mathscr{P}$	point on the horizontal working plane
P_v	parallel solar beam illuminance on the horizontal plane (lx)
$p_D(\vartheta, \phi, \Theta, \Phi)$	normalized scattering function
q	ratio of the illuminated diffuser element to the illuminated dome element
R	radius of the tube (m)
$R_{\mathrm{d}\sigma}$	distance from the diffuser element to the working plane element (m)
$\mathfrak{R}_{\mathrm{S}}$	angular radius of the Sun disk
r_0	distance between the diffuser element and centre of the diffuser (m)
r_1	distance of the first point of the reflection from surface element of the diffuser (m)
T_v	luminous turbidity factor in the direction of sun-beams
t_{C}	transmission coefficient of the cupola/dome
t_{D}	transmission coefficient of the diffuser
$X_{\mathrm{D}}, Y_{\mathrm{D}}, Z_{\mathrm{D}}$	position of the diffuser centre (in the coordinate system of the room)
X', Y', Z'	position of the point on the horizontal working plane (in the coordinate system of the room)
x_0, y_0, z_0	position of the target point on the diffuser (in the coordinate system of the diffuser)
x_1, y_1, z_1	coordinates of the first point of the reflection (in the coordinate system of the diffuser)

Greek symbols

α	exterior azimuth angle of the sky element
α_{room}	azimuth of X-axis of the room
α_{S}	azimuth of the Sun
γ_{S}	solar altitude
ε	eccentricity factor
ζ	zenith angle of the sky element
ζ_{S}	solar zenith angle
ϑ	zenith angle of the incident/reflected beam in the tube
Θ	zenith angle of the beam directed to the point of the working plane
ρ	interior surface reflectance of the light-tube
σ	total surface of the diffuser
$\mathrm{d}\sigma$	surface element on the diffuser
Φ	horizontal (polar) angle between evaluated point $\mathscr{P}$ and x-axis (in plan)
ϕ	azimuth of the incident/reflected sky beam in the tube
$\phi^{(i)}$	azimuth of the incident/reflected sun beam in the tube
ϕ_0	polar angle between diffuser element and x-axis of the diffuser
$\varphi(0)$	luminance gradation function for sky element in zenith
$\varphi(Z)$	luminance gradation function for sky element with zenith angle Z
χ	angular distance between sky element and sun position

– the multiple interreflection passes within the light-tube,

– the scattering properties of the diffuser itself resulting in directional luminance distribution into the interior space,

– the calculation method to derive the resulting distribution on a horizontal plane of the illuminated interior.

There are many indications in several publications that such a theoretical analytical approach was avoided due to many difficulties and uncertainties for computer programming as well as for the performance assessment criteria. Therefore several studies and experiments containing either measurements of prototype tubes or their installations in real interiors were investigated and published (Harrison et al., 1998; Oakley et al., 2000; Carter, 2002).

The first studies of the light transmittance trough light-pipe systems based on the light flux calculations tried to develop methods for prediction of tube transmission efficiency (Swift and Smith, 1995; Shao et al., 1997) and later interior illuminance (Zhang et al., 2002; Jenkins et al., 2005). Also programs Radiance, Superlite and SkyVision were used to evaluate vertical and horizontal illuminances as well as daylight factors in the selected interiors (Bracale et al., 2001; Laouadi, 2004).

CIE (2005) contains some case studies with measured external and interior illuminance measurements under three different sky conditions, e.g. clear with sunlight, cloudy or intermediate and overcast. All cases are compared in Daylight Factor percentages. Furthermore in Appendix C in the above CIE Report a TTE – Tube transmission efficiency formula was suggested depending on the so called "aspect ratio H/D", i.e. equivalent optical length H to tube diameter D and reflectance ρ. These few practical trials indicate the necessity to take into account the light-guide performance and efficiency under different outdoor conditions, but use a suspect assessment criterion of the Daylight factor (DF), which is useful only when a standard overcast sky without any sunlight exists.

Earlier Zhang and Muneer (2000) proposed to use DPF – Daylight Penetration Factor relating the internal and total external illuminance with a light-pipe version of the DF characterising the transmittance of the tube in a particular interior point. In the design guide (Zhang et al., 2002) 15 light-pipes with the diffuser 2 m to the working plane were monitored in February, April and July at 10 a.m. under clear, part-overcast and overcast conditions at Kew, UK and internal illuminance in 0, 1 and 2 m distances from the plan centre of the tube are given in tables. In the appended discussion the authors concede that "for innovative daylighting devices and some of the new designs, especially those that utilise not only skylight but also sunlight, to date, no general method is available to assess their daylighting performance".

It is evident that the performance efficiency of hollow light guides is rising when direct sunlight can be redirected and dispersed in a dim interior and therefore their year-round energy effectiveness in different daylight climates is important.

2. Sunlight and skylight availability

The most powerful source of light on earth is sunlight which is defined at the outer border of the atmosphere either by the so called Luminous Solar Constant (LSC) or by average luminance of the Sun disk (Darula et al., 2005). The LSC value represents either the extraterrestrial luminous flux 133 334 lm/m^2 or the illuminance of a fictitious plane perpendicular to sun-beams, i.e. $E_{vo} = 133\,334$ lx. As the solid angle of the Sun disk from the atmospheric border is rather small corresponding to the angular width of roughly 32 angular minutes the average solar luminance is extremely high at about $L_{vo} = 1\,963\,530$ kcd/m^2 on equinox day. Due to the year-round changes of the distance between the Sun and Earth also daily LSC and L_{vo} values can be calculated due to the so called eccentricity correction factor of the earth's orbit ε (Iqbal, 1983). However, for ground level locales the illuminance on a horizontal extraterrestrial plane is usually normalising, thus

$$E_v = E_{vo}\varepsilon \sin \gamma_S = E_{vo}\varepsilon \cos \zeta_S \tag{1}$$

where

γ_S is the solar altitude

ζ_S is the solar zenith angle equal $\pi/2 - \gamma_S$

Sunlight illuminance at ground level on a horizontal plane in accordance to the Bouguer's law is

$$P_v = E_v \exp(-a_v m T_v) \tag{2}$$

where

a_v is the luminous extinction coefficient for pure molecular atmosphere (Rayleigh-case)

m the relative optical air mass of the atmosphere

T_v is luminous turbidity factor in the direction of sun-beams

All these influences can be taken in accordance with the Twin System (Darula and Kittler, 2006). When measurements of the global G_v and diffuse sky D_v illuminance data are available a set of parameters can be used to determine daylight climate at ground level (Darula and Kittler, 2002), i.e. $P_v = G_v - D_v$, as well as parameters P_v/E_v and D_v/E_v. Thus an actual value of the turbidity factor is determined

$$T_v = -\frac{\ln P_v/E_v}{a_v m} \tag{3}$$

Furthermore, typical luminance distribution is standardized by ISO (2004) and CIE, 2003 in relative terms, i.e. normalised to zenith luminance. The whole set of 15 sky types (Kittler et al., 1998) is generally based on the so called luminance gradation functions φ for the zenith angular distance of the sky element $\varphi(\zeta)$ and for the zenith itself $\varphi(0)$ as well as the scattering indicatrix function f for the shortest angular distance between the sky element and the sun position $f(\chi)$ and for its value of the solar zenith angle $f(\zeta_S)$. Thus the luminance of an arbitrary sky element L_a normalised to zenith luminance L_z is defined as

$$\frac{L_a}{L_z} = \frac{f(\chi)\varphi(\zeta)}{f(\zeta_S)\varphi(0)} \tag{4}$$

where

χ is angular distance between sky element and sun position equal to $\chi = \arccos[\cos\zeta_S\cos\zeta + \sin\zeta_S\sin\zeta\cos(\alpha - \alpha_S)]$

ζ_S the solar zenith angle

ζ the zenith angle of the sky element

α the azimuth angle of the sky element

α_S is solar azimuth angle

Both luminance gradation function $\varphi(\zeta)$ and $\varphi(0)$ parametrised by a and b as well as the scattering indicatrix functions $f(\chi)$ and $f(\zeta_S)$ with parameters c, d and e are standardised in ISO (2004) and CIE, 2003.

So zenith luminance in absolute values has to be specified in accordance to D_v/E_v and T_v values (Darula et al., 2006). Of course, if measured data are not available, then D_v/E_v and T_v can be estimated and applying the integration of the particular luminance pattern the D_v illuminance can be derived.

3. Theoretical calculation of the interior illuminance originated from skylight

The passive roof-light and hollow-light components typically collect exterior skylight and sunlight and transport both into interior rooms closed by a diffuser embedded in their ceilings (Fraas et al., 1983).

If sunlight is absent the illuminance $E_{i,D}$ of an infinitesimally small surface $d\sigma$ of the diffuser will be predetermined in a local coordinate system (Fig. 1), in which

$$E_{i,D}(\phi_0, r_0) = \int_{\vartheta=0}^{\pi/2}\int_{\phi=0}^{2\pi} j(\vartheta,\phi,\phi_0,r_0)\cos\vartheta\sin\vartheta\,d\vartheta\,d\phi \quad (5)$$

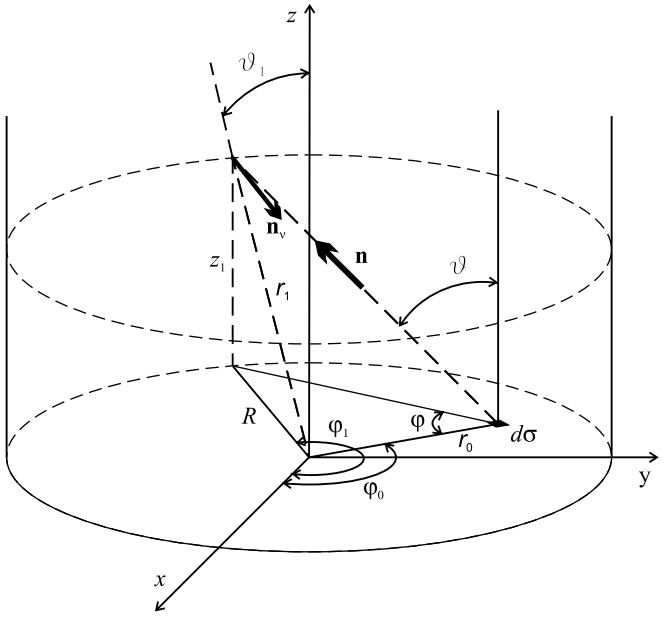

Fig. 1. Local diffuser coordinate system and parameters of rays incident on the diffuser.

where

$j(\vartheta,\phi,\phi_0,r_0)$ is the sky luminance producing illuminance on the diffuser element via the light-tube

ϕ_0 the polar angle, measured from x-axis toward y-axis in the counterclockwise direction

r_0 the radial distance of the elementary surface on the diffuser from the centre of circular diffuser

ϑ the apparent zenith angle of incident beam received at $d\sigma$

ϕ is azimuth angle of incident beam received at $d\sigma$

Because the diffuser lies in the horizontal plane, ϑ always corresponds to the real zenith angle (independently of position ϕ_0, r_0), but ϕ differs from the real (exterior) azimuth angle α. Contrary to ϕ_0, the angle α is measured in horizontal plane of the coordinate system from the North toward the East (i.e. clockwise). In such a case the polar angle ϕ_0, measured in a local coordinate system of the diffuser can be transformed into the exterior azimuth angle α as

$$\alpha = \alpha_{room} - \phi_0 \quad (6)$$

where α_{room} is the azimuth of X-axis of the room, Fig. 2. After transmission through the diffuser, the light is distributed into the interior room space. In general, the angular behaviour of the light emitted by the diffuser downward into the room depends on the direction of incidence ϑ, ϕ and on the direction of propagation Θ, Φ (Minin, 1988). While ϑ varies from 0 to $\pi/2$, the angle Θ is from $\pi/2$ to π.

The total illuminance of a working plane situated horizontally within the room is

$$E_{i,W}(X',Y',Z') = \frac{t_D}{\pi}\int_\sigma \frac{\cos^2\Theta}{R^2_{d\sigma}(\Theta,\Phi)} \left[\int_{\vartheta=0}^{\pi/2}\int_{\phi=0}^{2\pi} j(\vartheta,\phi,\phi_0,r_0)p_D(\vartheta,\phi,\Theta,\Phi)\cos\vartheta\sin\vartheta\,d\vartheta\,d\phi\right] d\sigma \quad (7)$$

where $\mathscr{P} = X', Y', Z'$ is the position at the working plane, t_D, $p_D(\vartheta,\phi,\Theta,\Phi)$, and σ are the transmission coefficient, normalized scattering function and total surface of the diffuser, respectively, and $R_{d\sigma}$ is a distance from elementary

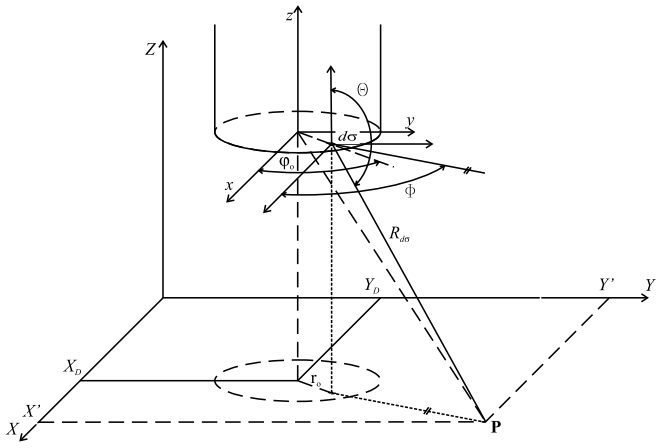

Fig. 2. Scheme of the placement of the tube in the room related to the working plane.

surface $d\sigma$ of the diffuser to the arbitrary evaluation point $\mathscr{P}$. Note that $d\sigma\cos(\pi-\Theta)/R^2_{d\sigma}(\Theta,\Phi)$ is an elementary solid angle subtended by $d\sigma$ at the point $\mathscr{P}$. For circular diffusers with radius R Eq. (7) reads

$$E_{i,W}(X',Y',Z') = \frac{t_D}{\pi}\int_0^R r_0 dr_0 \int_0^{2\pi} \frac{\cos^2\Theta}{R^2_{d\sigma}(\Theta,\Phi)} d\phi_0 \int_0^{\pi/2} \cos\vartheta \times \sin\vartheta\, d\vartheta \int_0^{2\pi} j(\vartheta,\phi,\phi_0,r_0) p_D(\vartheta,\phi,\Theta,\Phi) d\phi \quad (8)$$

because $d\sigma = r_0 dr_0 d\phi_0$. The factor $\cos^2\Theta$ occurs because both, the diffuser as well as the illuminated surface, lie in the horizontal plane. If either slope of the diffuser Θ_D or slope of the working plane Θ_W differ from the horizontal position ($\neq\pi/2$), the factor $\cos^2\Theta$ has to be replaced by $\cos[\pi - B(\Theta,\Theta_D)]\cos[\pi - B(\Theta,\Theta_W)]$. Here $B(\Theta,\Theta_D)$ is a non-trivial function depending on system geometry. When e.g. the diffuser and the working plane would turn around axes x and X respectively, and the illuminance is measured along axis Y (i.e. Y' varies freely, while X' is fixed) the factor will acquire form: $\cos(\pi/2-\Theta+\Theta_D)\cos(\pi/2-\Theta+\Theta_W)$.

Further the diffuser and working surface will be considered to lie in horizontal position using X_D, Y_D, Z_D for coordinates of the centre of the diffuser (see Fig. 2), then the distance $R_{d\sigma}$ can be found from

$$R_{d\sigma} = \sqrt{(X'-X_D-r_0\cos\phi_0)^2 + (Y'-Y_D-r_0\sin\phi_0)^2 + (Z'-Z_D)^2} \quad (9)$$

The angles Θ, Φ characterising the scattering direction are obtained from the following equations:

$$\cos\Theta = \frac{Z'-Z_D}{R_{d\sigma}}$$
$$\sin\Theta\cos\Phi = \frac{X'-X_D-r_0\cos\phi_0}{R_{d\sigma}} \quad (10)$$
$$\sin\Theta\sin\Phi = \frac{Y'-Y_D-r_0\sin\phi_0}{R_{d\sigma}}$$

Considering the Lambertian diffuser (Maradudin et al., 2003), the quantity $p_D(\vartheta,\phi,\Theta,\Phi)$ does not depend on directions of the incoming and outgoing beam, i.e. $p_D(\vartheta,\phi,\Theta,\Phi)\equiv 1$ and thus

$$E_{i,W}(X',Y',Z') = \frac{t_D}{\pi}\int_0^R r_0 dr_0 \int_0^{2\pi} \frac{\cos^2\Theta}{R^2_{d\sigma}(\Theta,\Phi)} d\phi_0 \times \int_0^{\pi/2} \cos\vartheta\sin\vartheta\, d\vartheta \int_0^{2\pi} j(\vartheta,\phi,\phi_0,r_0) d\phi \quad (11)$$

instead of Eq. (7). Having defined both the optical characteristics of the diffuser (i.e. $p_D(\vartheta,\phi,\Theta,\Phi)$ and t_D) and geometrical relations (i.e. the position of the centre of circular diffuser X_D, Y_D, Z_D) the illuminance in any point $\mathscr{P} = X',Y',Z'$ can be calculated. Now there is still an unknown quantity, i.e. the luminance $j(\vartheta,\phi,\phi_0,r_0)$ reaching the diffuser from the sky after multiple reflections in the light-tube.

4. Multiple reflections in the cylindrical light-tube

When the sunlight is absent the luminance $j(\vartheta,\phi,\phi_0,r_0)$ reaching the elementary surface $d\sigma$ of the diffuser (having the position ϕ_0, r_0) is a product of three functions

$$j(\vartheta,\phi,\phi_0,r_0) = L(\zeta,\alpha-\alpha_S)\rho^N t_C = L_a(\zeta,\zeta_S,\chi,L_Z)\rho^N t_C = L_a\rho^N t_C \quad (12)$$

where

- $L(\zeta,\alpha-\alpha_S)$ is sky luminance positioned on the sky hemisphere
- ζ the zenith angle
- α the azimuth angle of a sky element which illuminates the surface $d\sigma$ from apparent direction ϑ, ϕ
- α_S the azimuth angle of the Sun
- ρ the reflectance of the interior surface of the light-tube which is considered to be independent of angle of incidence
- t_C is cupola transmission coefficient

Both ζ and α represent the entry-direction from which the scattered natural light acts on the cupola mounted on the top of the light-tube. It is evident that the final direction of the incident light on the diffuser has relation to the entry-direction ζ and α (depending on tube geometry and orientation of the room in respect to the Sun) so in general, $\zeta\equiv\zeta(\vartheta,\phi,\phi_0,r_0)$ and also $\alpha\equiv\alpha(\vartheta,\phi,\phi_0,r_0)$. Usually the value of ρ is close to 1, e.g. mirror light guides are using surfaces with ρ roughly 0.98. If a beam undergoes N reflections inside the light-tube until it reaches the diffuser, the original luminance is reduced by a factor ρ^N. The dome mounted at the top of roof-light is typically made from very transparent materials (like glass or Plexiglas) so t_C is usually between 0.8 and 0.92. The evaluation of the function $j(\vartheta,\phi,\phi_0,r_0)$ requires to determine three unknown parameters: ζ, α, and N.

4.1. Methodological approach

The Cartesian coordinates of the target point $\mathscr{P}$ in which the beam hits the elementary surface $d\sigma$ of the diffuser are written as follows:

$$x_0 = r_0\cos\phi_0$$
$$y_0 = r_0\sin\phi_0 \quad (13)$$
$$z_0 = 0$$

while the coordinates of the first point of reflection (in the backwards direction to beam incidence, i.e. from the diffuser toward the cupola) are

$$x_1 = r_1\cos\phi_1\sin\vartheta_1$$
$$y_1 = r_1\sin\phi_1\sin\vartheta_1 \quad (14)$$
$$z_1 = r_1\cos\vartheta_1$$

The radial distance r_1, and angles ϑ_1 and ϕ_1 are functions of ϑ, ϕ, ϕ_0, r_0 and R, Fig. 1. In accordance to the Sine law is

$$\phi_1 = \phi_0 - \phi + \pi - \arcsin\left(\frac{r_0}{R}\sin\phi\right) \tag{15}$$

and consequently ϑ_1 and r_1 are obtained as

$$\tan\vartheta_1 = \tan\vartheta\frac{\sin\phi}{\sin(\phi_1-\phi_0)}; \quad r_1 = \frac{R}{\sin\vartheta_1} \tag{16}$$

Both direct sky luminance within small solid angles and multiple reflected skylight and occasional sunlight contribute to the illunminance of the diffuser. Therefore it is advantageous to solve the problem in reverse directions and use the backward ray-tracing approach. Furthermore, it is evident that the vector analysis is quite feasible.

Eqs. (15) and (16) are basis for derivation of the unit vector along the first upward direction

$$\mathbf{n}_1 = \frac{1}{\sqrt{(x_1-x_0)^2+(y_1-y_0)^2+(z_1-z_0)^2}} \times [(x_1-x_0),(y_1-y_0),(z_1-z_0)] \tag{17}$$

To find the unit vector $\mathbf{n}_2$ after the first "reversed" reflection the unit vector $\mathbf{n}_v$ in the normal direction to the surface of the cylinder has to be defined. It is easy to express it as

$$\mathbf{n}_v = (-\cos\phi_1, -\sin\phi_1, 0) \tag{18}$$

The law of reflection guarantees that unit vectors $\mathbf{n}_1$, $\mathbf{n}_v$ and $\mathbf{n}_2$ must lie in the same plane and the angles of incidence and reflection must be equal. This is fulfilled when vector products as well as dot products of above mentioned unit vectors satisfy the following conditions:

$$\begin{aligned}\mathbf{n}_v\times\mathbf{n}_1 &= \mathbf{n}_v\times\mathbf{n}_2\\ \mathbf{n}_2\cdot\mathbf{n}_v &= -\mathbf{n}_1\cdot\mathbf{n}_v\end{aligned} \tag{19}$$

The system of Eqs. (19) is satisfactory to obtain $\mathbf{n}_2$ by means of $\mathbf{n}_1$ and $\mathbf{n}_v$. However, another more convenient approach is to decompose $\mathbf{n}_1$ and $\mathbf{n}_2$ into two vectors

$$\begin{aligned}\mathbf{n}_1 &= \mathbf{n}_1' + \mathbf{n}_1''\\ \mathbf{n}_2 &= \mathbf{n}_2' + \mathbf{n}_2''\end{aligned} \tag{20}$$

with $\mathbf{n}_1''$ and $\mathbf{n}_2''$ parallel to $\mathbf{n}_v$. Then

$$\mathbf{n}_1'' = (\mathbf{n}_1\cdot\mathbf{n}_v)\mathbf{n}_v = -\mathbf{n}_2'' \tag{21}$$

and $\mathbf{n}_1' = \mathbf{n}_2'$ (respecting the law of reflection). Finally is

$$\mathbf{n}_2 = \mathbf{n}_1 - 2(\mathbf{n}_1\cdot\mathbf{n}_v)\mathbf{n}_v \tag{22}$$

Any further points of the intersection of a beam with the cylindrical light-tube in the backward direction are calculated recurrently:

$$\begin{aligned}x_i &= k_i(\mathbf{n}_i)_x + x_{i-1}\\ y_i &= k_i(\mathbf{n}_i)_y + y_{i-1} \quad i>1\\ z_i &= k_i(\mathbf{n}_i)_z + z_{i-1}\end{aligned} \tag{23}$$

The coefficient of proportionality k_i is found from the condition $(x_i^2+y_i^2) = R^2$. Eq. (22) will be used recurrently to determine $\mathbf{n}_i = \mathbf{n}_{i-1} - 2(\mathbf{n}_{i-1}\cdot\mathbf{n}_v)\,\mathbf{n}_v$, where $\mathbf{n}_v = (-\cos\phi_{i-1}, -\sin\phi_{i-1}, 0)$ and $i>1$. Both specific forms of the vector $\mathbf{n}_v$ (for the vertically situated cylindrical light-tube) and Eq. (21) guarantee that angle ϑ is conserved in the process of internal reflections. The loop is terminated when z_i exceeds H, where H is the height of the vertical cylindrical tube. Number of reflection events is then $N = i-1$. Because the pair (ϑ,ϕ_{N+1}) is understood as the direction of incidence in the far-field zone approximation, the unit vector $\mathbf{n}_{N+1}$ can be shifted arbitrarily without having any effect on the resulting (ϑ,ϕ_{N+1}). Positioning $\mathbf{n}_{N+1}$ into centre of the coordinate system of the diffuser it can be expressed as

$$\mathbf{n}_{N+1} = (\cos\phi_{N+1}\sin\vartheta, \sin\phi_{N+1}\sin\vartheta, \cos\vartheta) \tag{24}$$

Using the transformation between local and horizontal coordinate systems after Eq. (6) the real azimuth of a sky element (found in accordance with the described ray-tracing approach) is $\alpha = \alpha_{\text{room}} - \phi_{N+1}$. Components $(\mathbf{n}_{N+1})_x$, $(\mathbf{n}_{N+1})_y$, $(\mathbf{n}_{N+1})_z$ are known from the last step of the recurrent scheme, and thus both $\zeta = \vartheta$, as well as $\alpha = \alpha_{\text{room}} - \phi_{N+1}$ can be obtained from Eq. (24).

4.2. Analytical solution

Principles and methods described in previous sections can be applied for hollow light guides having various well defined geometrical forms (like those presented in Gupta et al. (2001)). The generalisation of above described approach depends on the correct expression of the local normal $\mathbf{n}_v$ to the surface of the light-tube, which can be a non-trivial task for light-tubes having complex shapes. The determination of the coefficients of proportionality k_i after text below Eq. (23) can also result in some difficulties, as $(x_i^2+y_i^2) = R^2$ is valid only for cylindrical objects. Therefore the radius R in Eqs. (15) and (16) must be replaced by a function corresponding to the form of the actual light-tube. However, the cylindrical light-tube having a horizontally positioned diffuser at the bottom and equipped by the hemispherical copula at the top represents a well-arranged system suitable to find an analytical solution.

Due to geometrical relations both the zenith angle of the sky element ζ and the apparent zenith angle ϑ (defined in the coordinate system of the diffuser) match together (i.e. $\zeta = \vartheta$). The solutions for azimuth angle of any sky element α and the number of interior reflections in the light-tube N are sought in two steps depending on the value of

$$h(\phi_0;\phi,\vartheta) = \frac{R}{\tan\vartheta}\frac{\sin(\phi_1-\phi_0)}{\sin\phi} \tag{25}$$

1. If $h(\phi_0;\phi,\vartheta) > H$, then $N(r_0,\phi_0;\phi,\vartheta)\equiv 0$ and

$$\alpha = \alpha_{\text{room}} - \phi_0 + \phi - \pi \tag{26}$$

2. Otherwise, if $h(\phi_0;\phi,\vartheta) \leqslant H$

$$\alpha = \alpha_{\text{room}} - N(r_0,\phi_0;\phi,\vartheta)\psi(r_0,\phi_0;\phi) - \phi_0 + \phi - \pi \tag{27}$$

where the number of reflections within the interior of light-tube is

$$N(r_0,\phi_0;\phi,\vartheta) = 1 + \text{Int}\left\{\frac{1}{2g(r_0,\phi_0;\phi)} \times \left[\frac{H\tan\vartheta}{R} - \frac{\sin(\phi_1-\phi_0)}{\sin\phi}\right]\right\} \tag{28}$$

The operand Int applied to any real value returns the truncated whole number (e.g. $\text{Int}(3.254) = 3$). The angle $\phi_1 \equiv \phi_1(r_0,\phi_0;\phi)$ is given by Eq. (15) and

$$g(r_0,\phi_0;\varphi) = s(r_0,\phi_0;\phi) + \cos(\phi_0-\phi)\cos\phi_1 + \sin(\phi_0-\phi)\sin\phi_1 \tag{29}$$

The function $s(r_0,\phi_0;\phi)$ reads

$$s(r_0,\phi_0;\phi) = \frac{2\sin\phi}{\sin(\phi_1-\phi_0)}\left[1 - \frac{r_0}{R}(\cos\phi_0\cos\phi_1 + \sin\phi_0\sin\phi_1)\right] \tag{30}$$

$$\psi(r_0,\phi_0;\phi) = \tilde{\phi} - \phi_0 + \phi - \pi \tag{31}$$

The angle $\tilde{\phi}$ can be obtained from the following two equations:

$$\begin{aligned}\cos\tilde{\phi} &= \cos(\phi_0+\pi-\phi) - s(r_0,\phi_0;\phi)\cos\phi_1\\ \sin\tilde{\phi} &= \sin(\phi_0+\pi-\phi) - s(r_0,\phi_0;\phi)\sin\phi_1\end{aligned} \tag{32}$$

It is necessary to deal with both equations whereas the inverse functions $\arccos(\tilde{\phi})$ and $\arcsin(\tilde{\phi})$ are ambiguous. Simultaneous evaluation of $\cos\tilde{\phi}$ and $\sin\tilde{\phi}$ leads to correct interpretation of the angle $\tilde{\phi}$. Strictly said, if $\cos\tilde{\phi} < 0$ then $\tilde{\phi} = \pi - \arcsin(\tilde{\phi})$, otherwise $\tilde{\phi} = \arcsin(\tilde{\phi})$ for $\sin\tilde{\phi} > 0$, and $\tilde{\phi} = 2\pi + \arcsin(\tilde{\phi})$ for $\sin\tilde{\phi} < 0$. This approach must be incorporated into the numerical scheme. Anyway, the inversion goniometric functions need to be always dealt with carefully. Typical example is a value of ψ obtained from Eq. (31): if namely $\psi < 0$ Eq. (31) must be transformed to $\psi(r_0,\phi_0;\phi) = \tilde{\phi} - \phi_0 + \phi + \pi$, i.e. $\psi + 2\pi$ is considered instead of ψ, simply because ψ is required to be positive in Eq. (27).

4.3. The contribution of direct solar beams

In general, the direct sunlight may also contribute to the illuminance on elementary surfaces $\mathrm{d}\sigma$ of the diffuser. If however, $\mathrm{d}\sigma$ is illuminated by light originated from sky element (ζ,α), which coincides with the position of the Sun (ζ_S,α_S), Eq. (11) for interior illuminance has to be extended by an additional term expressing sunlight contribution, i.e.

$$\begin{aligned}E_{i,W}(X',Y',Z') = {} & \frac{t_D}{\pi}\int_0^R r_0\mathrm{d}r_0\int_0^{2\pi}\frac{\cos^2\Theta}{R^2_{d\sigma}(\Theta,\Phi)}\mathrm{d}\phi_0 \times \int_0^{\pi/2}\cos\vartheta\sin\vartheta\,\mathrm{d}\vartheta\int_0^{2\pi} j(\vartheta,\phi,\phi_0,r_0)\mathrm{d}\phi\\ & + \frac{t_D t_C}{\pi}\int_0^R r_0\mathrm{d}r_0\int_0^{2\pi}\frac{\cos^2\Theta}{R^2_{d\sigma}(\Theta,\Phi)} \times \left(\sum_{i=1}^{M} P_V \rho^{N_{\text{Sun}}(\phi^{(i)})}\left|\frac{\mathrm{d}\alpha(r_0,\phi_0;\phi,\zeta_S)}{\mathrm{d}\phi}\right|^{-1}_{\phi^{(i)}}\right)\mathrm{d}\phi_0\end{aligned} \tag{33}$$

where P_V is the exterior illuminance on a horizontal surface due to direct sunlight.

The number of reflections of sun-beams $N_{\text{Sun}}(\phi^{(i)}) \equiv N(r_0,\phi_0;\phi^{(i)},\zeta_S)$ is obtained from Eq. (28) when substituting $\vartheta = \zeta_S$. Otherwise $N_{\text{Sun}}(\phi^{(i)})$ is zero by definition when $h(\phi_0;\phi^{(i)},\zeta_S) > H$. Because the light-tube represents a quite complex optical system, the direct sun-beams can, in principle, reach $\mathrm{d}\sigma$ from M different directions $\phi^{(1)}\ldots\phi^{(M)}$. Due to many interreflections the local maxima (or minima) of illumination patches on the diffuser can occur (Swift et al., 2006). If the sunlight undergoes only one reflection event (in case of a small height H of the light tube) the inversed focused image of the Sun should be observed in position $\phi_0 = \pi + \alpha_{\text{room}} - \alpha_S$ on the diffuser. Total contribution of the sunlight to the illumination of the given surface element $\mathrm{d}\sigma$ of the diffuser is obtained as a sum over all M directions of incidence. For a fixed r_0, and ϕ_0 all independent solutions $\phi^{(1)}\ldots\phi^{(M)}$ can be retrieved from the following equation:

$$\alpha_S = \alpha_{\text{room}} - N(r_0,\phi_0;\phi^{(i)},\zeta_S)\psi(r_0,\phi_0;\phi^{(i)}) - \phi_0 + \phi^{(i)} - \pi \tag{34}$$

If $N_{\text{Sun}} = 0$, see Eq. (26), there exists only one unique solution because simply $\phi^{(1)} = \alpha_S - \alpha_{\text{room}} + \phi_0 + \pi$. Although apparent zenith angle ϑ is conserved during processes of multiple reflections it must be highlighted that there is an evident discrepancy between apparent azimuth angle ϕ (measured in local coordinate system of the diffuser) and entry (exterior) azimuth α. Consequently the elementary solid angle $\sin\vartheta\,\mathrm{d}\vartheta\,\mathrm{d}\phi$ measured at the diffuser differs from solid angle $\sin\vartheta\,\mathrm{d}\vartheta\,\mathrm{d}\alpha$ at the top of the roof-light. Therefore the surfaces illuminated by sun-beams at the top of dome $\mathrm{d}\sigma^{\text{top}}$ and at the diffuser $\mathrm{d}\sigma$ are not the same. Because the sun-beams are propagating from infinity toward diffuser the equality $\mathrm{d}\alpha/\mathrm{d}\phi = \mathrm{d}\sigma/\mathrm{d}\sigma^{\text{top}}$ is valid. Note that enlargement of the illuminated surface by a factor $q = \mathrm{d}\sigma/\mathrm{d}\sigma^{\text{top}}$ $(q > 1)$ results in reduction of the local illuminance, i.e. illuminance is proportional to $1/q$. If no reflections in the light-tube occur the illuminated surface must be conserved, i.e. $q = 1$. This fact can be easily justified when calculating a derivative of Eq. (26)

$$\frac{\mathrm{d}\alpha(\phi_0;\phi)}{\mathrm{d}\phi} = \frac{\mathrm{d}\sigma}{\mathrm{d}\sigma^{\text{top}}} = 1 \tag{35}$$

The derivative $\mathrm{d}\alpha/\mathrm{d}\phi$ can be expressed analytically also when the number of interior reflections $N_{\mathrm{Sun}}(\phi^{(i)}) \geqslant 1$

$$\begin{aligned}\frac{\mathrm{d}\alpha(r_0,\phi_0;\phi,\zeta_S)}{\mathrm{d}\phi} &= 1+\frac{N_{\mathrm{Sun}}}{\cos\tilde{\phi}}\left[s\left(1+\frac{\mathrm{d}\phi_1}{\mathrm{d}\phi}\right)\cos\phi_1+\frac{\mathrm{d}s}{\mathrm{d}\phi}\sin\phi_1\right]\\ &+\psi\mathrm{Int}\left\{\frac{Q}{2g^2}\left(1+\frac{\mathrm{d}\phi_1}{\mathrm{d}\phi}\right)[\sin(\phi_0-\phi)\cos\phi_1\right.\\ &-\cos(\phi_0-\phi)\sin\phi_1]+\frac{Q}{2g^2}\frac{\mathrm{d}s}{\mathrm{d}\phi}\\ &+\frac{1}{2g\sin\phi}\left[\frac{\mathrm{d}\phi_1}{\mathrm{d}\phi}\cos(\phi_1-\phi_0)\right.\\ &\left.\left.-\sin(\phi_1-\phi_0)\cot\phi\right]\right\} \end{aligned} \tag{36}$$

where for simplicity the following denotations were applied: $N_{\mathrm{Sun}} \equiv N(r_0,\phi_0;\phi^{(i)},\zeta_S)$, $\phi_1 \equiv \phi_1(r_0,\phi_0;\phi)$, $s \equiv s(r_0,\phi_0;\phi)$, and $g \equiv g(r_0,\phi_0;\phi)$. The derivative of Eq. (36) is evaluated for all those $\phi = \phi^{(i)}$ which represent a complete set of solutions of Eq. (34). The function $Q \equiv Q(\phi_0;\phi,\vartheta)$ used in Eq. (36) has the form

$$Q = \frac{H\tan\vartheta}{R} - \frac{\sin(\phi_1-\phi_0)}{\sin\phi} \tag{37}$$

while the rest derivatives can be obtained as

$$\frac{\mathrm{d}\phi_1}{\mathrm{d}\phi} = -1 - \frac{r_0\cos\phi}{\sqrt{R^2-r_0^2\sin^2\phi}} \tag{38}$$

and

$$\begin{aligned}\frac{\mathrm{d}s}{\mathrm{d}\phi} &= s\left[\cot\phi-\frac{\mathrm{d}\phi_1}{\mathrm{d}\phi}\cot(\phi_1-\phi_0)\right]-\frac{\mathrm{d}\phi_1}{\mathrm{d}\phi}\\ &\times\frac{2\sin\phi[\sin\phi_0\cos\phi_1-\cos\phi_0\sin\phi_1]}{\sin(\phi_1-\phi_0)}\frac{r_0}{R}\end{aligned} \tag{39}$$

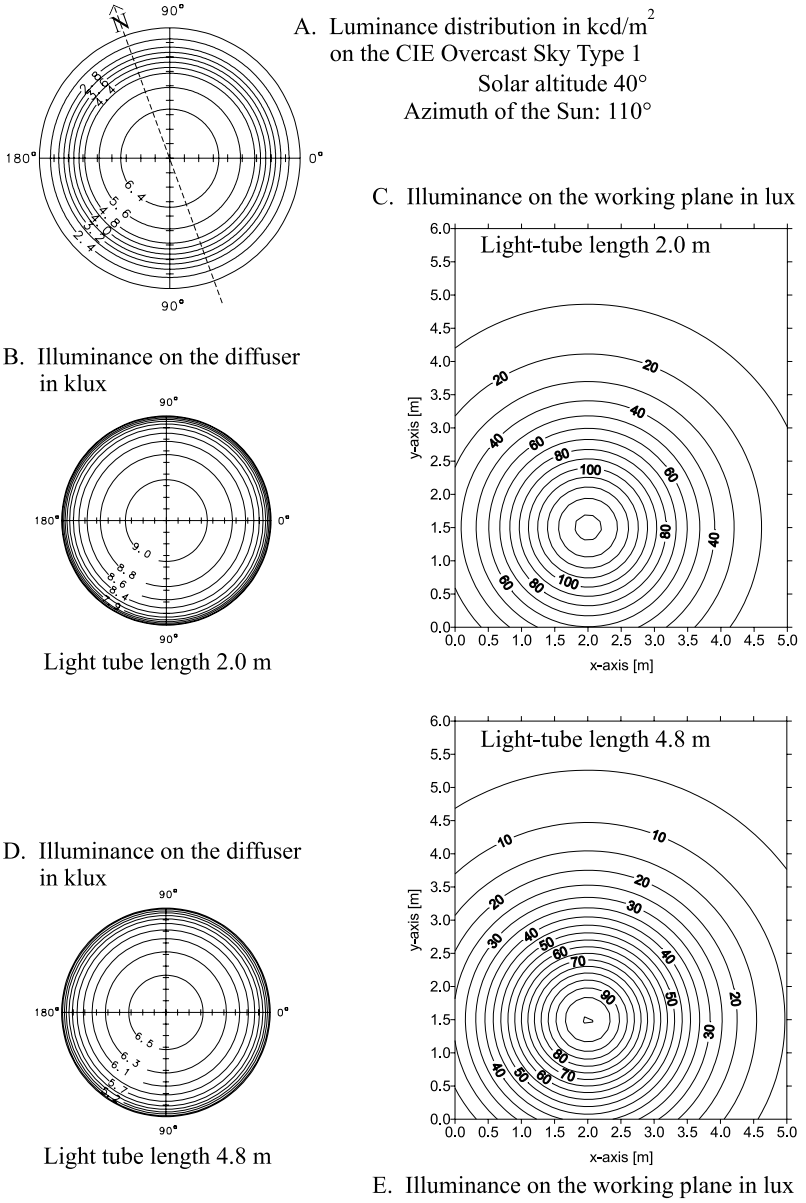

Fig. 3. Example of illuminance distribution on the diffuser and working plane under CIE Overcast Sky conditions and 2.0 or 4.8 m tube lengths.

An alternative approach how to incorporate the sunlight into the model can be based on the representation of the Sun as a finite-dimensional luminous source with an extra-terrestrial luminance L_{vo} which is seen at ground level reduced by the transmission of the atmosphere as

$$L_S = L_{vo}\exp(-a_v m T_v) \tag{40}$$

thus

$$j_S(\vartheta,\phi,\phi_0,r_0) = L_S \rho^{N_{Sun}(\phi)} t_C \tag{41}$$

However, as the solar extraterrestrial luminance and illuminance are interrelated (Darula et al., 2005) also the solar luminance and illuminance at ground level are proportionally normalised by the sun solid angle, then

$$j_S(\vartheta,\phi,\phi_0,r_0) = \frac{P_V}{\cos\zeta_S}\frac{\rho^{N_{Sun}(\phi)} t_C}{2\pi(1-\cos\Re_S)} \tag{42}$$

where

$P_V/\cos\zeta_S$ is the exterior illuminance received at the plane normal to the incident sun-beams

$\Re_S$ is angular radius of the Sun disk from ground level which is 16 angular minutes

The distribution of the illuminance on the diffuser is then expressed in a more compact form

$$E_{i,W}(\phi_0,r_0) = \int_{\vartheta=0}^{\pi/2}\int_{\phi=0}^{2\pi} j_T(\vartheta,\phi,\phi_0,r_0)\cos\vartheta\sin\vartheta\,d\vartheta\,d\phi \tag{43}$$

The luminance $j_T(\vartheta,\phi,\phi_0,r_0) = j(\vartheta,\phi,\phi_0,r_0) + j_S(\vartheta,\phi,\phi_0,r_0)$ when angular distance of the sky element (characterized by coordinates ϑ, ϕ) from the centre of the Sun disk (with coordinates ξ_S, α_S) is smaller than $\Re_S$. In all other cases $j_T(\vartheta,\phi,\phi_0,r_0) = j(\vartheta,\phi,\phi_0,r_0)$, where luminance $j(\vartheta,\phi,\phi_0,r_0)$ is given by Eq. (12). Nevertheless, the calculation scheme based on Eq. (43) is impractical because it requires a very dense grid $\vartheta\times\phi$ with small lattice-spacing $d\vartheta$ and $d\phi$. Such numerical calculations are time-consuming. On the other hand, the analytical approach formulated by Eqs. (33)–(39) is rigorous, very efficient, accurate and extremely powerful. In addition, the analyticity of the solution reveals close mathematical ties with propagation of the light through cylindrical light-tubes and results in efficient incorporation of the sunlight into the model for calculating the optical characteristics of the hollow light guides.

5. Numerical examples under overcast and clear sky conditions

Using the above method and formulae any standard sky luminance pattern (or any physically-justified sky radiance model – see e.g. Kocifaj and Lukáč, 1998) could be applied to calculate resulting illuminances either on the hollow tube diffuser or on the working plane of the interior. Therefore a special computer program was developed to test HOLIGILM in several examples. To demonstrate this application two critical luminance patterns were chosen, i.e. overcast sky pattern for the CIE Overcast Sky with sunlight absent and a clear sky pattern, namely the CIE Clear Sky with the Sun in a chosen position.

To introduce the examples several further assumptions have to be stated, e.g.:

- Dimensions and parameters of the hollow light guide (Bracale et al., 2001; Carter, 2002; Plch and Mohelnikova, 2005a; Plch and Mohelnikova, 2005b):
  - the radius of the tube $R = 0.26$ m,
  - height of the cylinder is varied $H = 0.5$, 1, 2 and 4.8 m,
  - reflectance of the light-tube $\rho = 0.934$,
  - transmission coefficient of the hemispherical cupola/dome $t_C = 0.92$,
  - transmission coefficient of the Lambertian diffuser $t_D = 0.75$,
- Dimensions of the interior:
  - room length in direction of the X-axis is 5 m,
  - room depth along the Y-axis is 6 m,
  - azimuthal orientation of the X-axis is 20°,
  - normal distance of the working plane from the diffuser is 2 m.

In the first example the overcast sky luminance distribution after ISO 15469:2004 sky type 1 corresponding to the CIE Overcast Sky was used. Assuming the diffuse to extraterrestrial horizontal illuminance $D_v/E_v = 0.2$ the

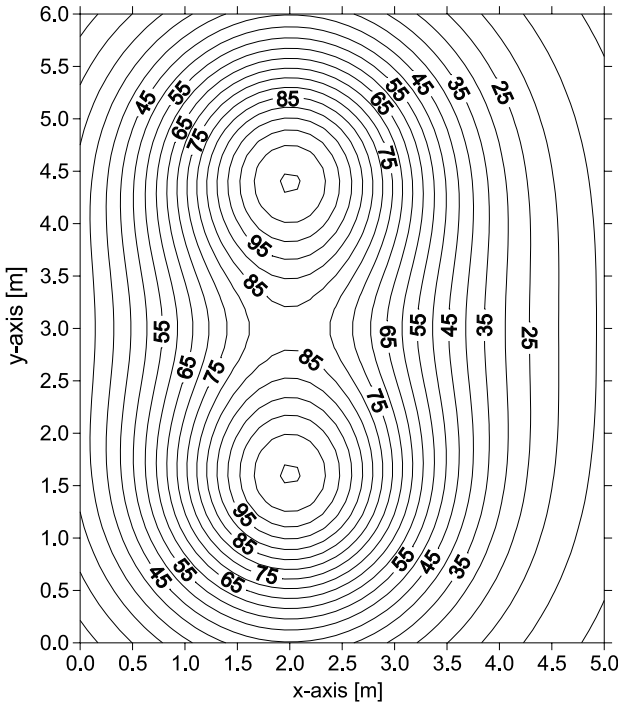

Fig. 4. Example of interior illuminance distribution with two 4.8 m tubes under CIE Overcast Sky.

resulting exterior illuminance is $D_v = 17.2$ klx under the solar zenith angle $\zeta_S = 50°$. Due to the fact that sunlight is excluded the luminance distribution is without dependence on the Sun position and azimuth changes, thus the luminance pattern is even and symmetrical around the zenith with a decreasing gradation towards horizon in Fig. 3A. This evenness is producing a similar illuminance distribution on the diffuser as shown in case of a 2 m long light-tube (Fig. 3B) and in case of a 4.8 m long tube with lower levels in Fig. 3D. In consequence of the Lambertian diffuser also the interior illuminance is evenly distributed on the working plane with a maximum under the centre of the diffuser. Of course, as expected higher illuminance levels are under the shorter 2 m tube (compare Fig. 3C and E). Although the D_v/E_v value and the sunheight are both relatively high the interior illuminanc-

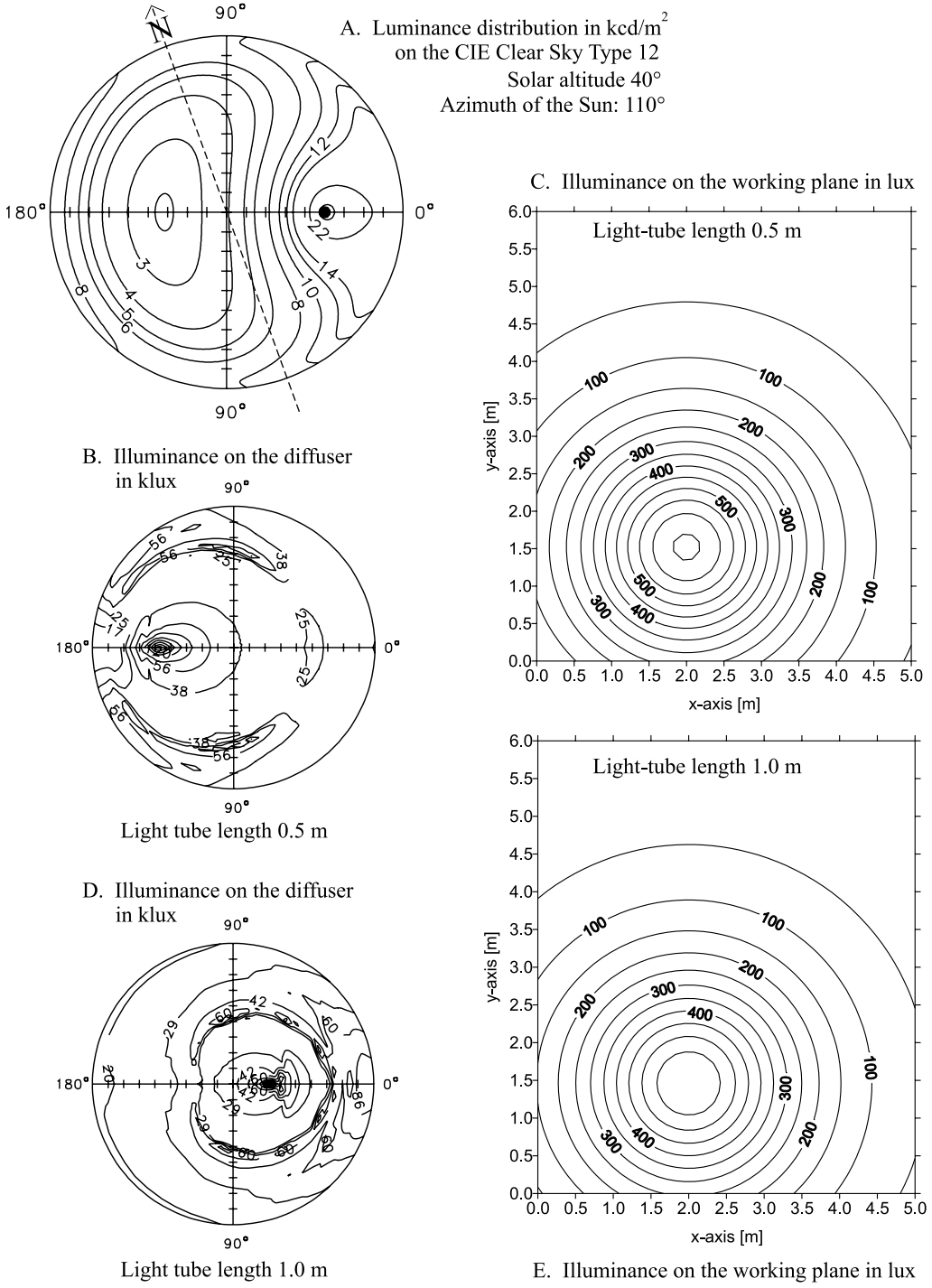

Fig. 5. Examples of illuminance distribution on the diffuser and working plane under CIE Clear Sky conditions: 0.5 or 1.0 m tube lengths (A–E); 2.0 or 4.8 m tube lengths (F–I).

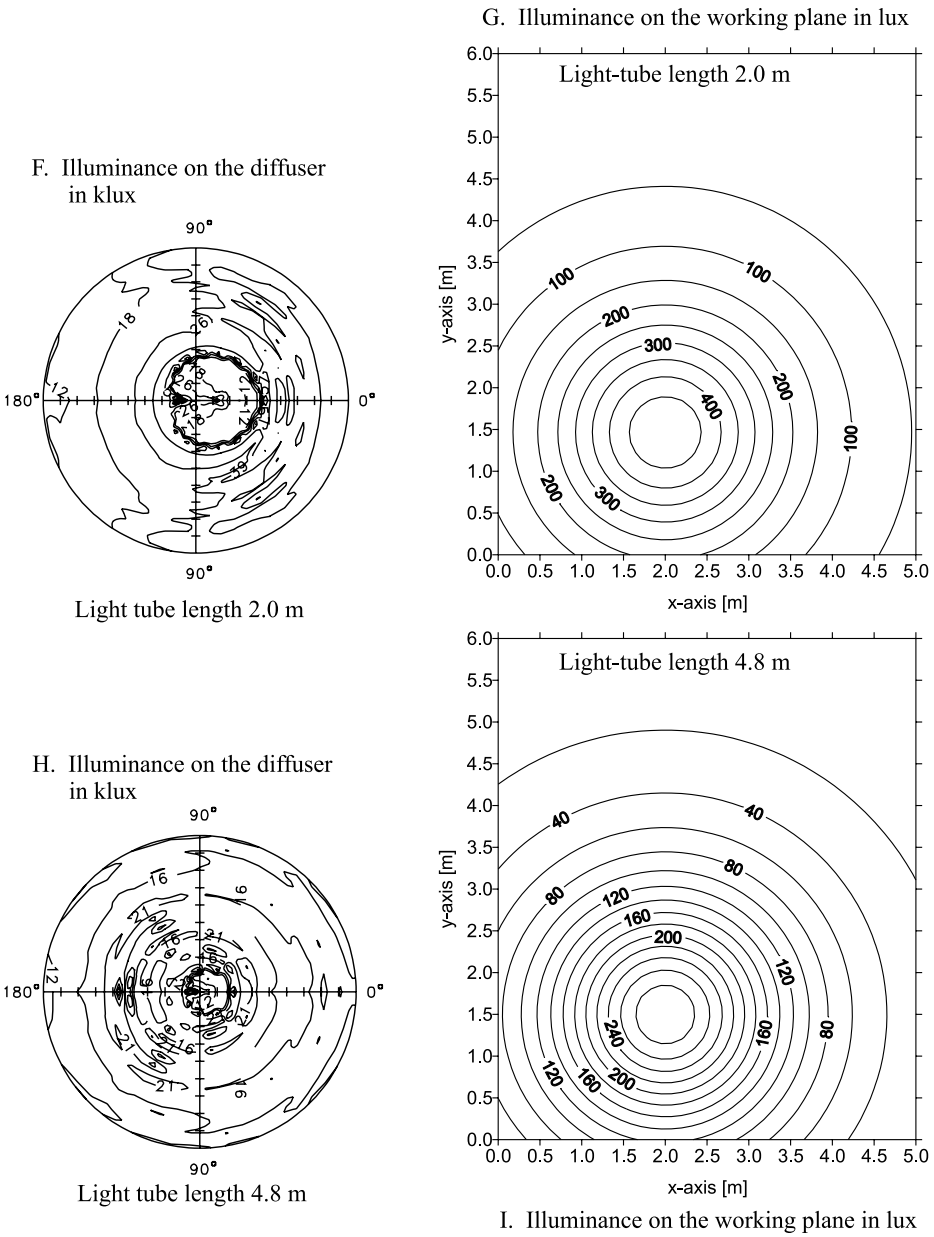

Fig. 5 (*continued*)

es are rather low and could be efficient only for visual orientation, e.g. in corridors or stores. In reality probably several hollow guide lines for instance two tubes with the 4.8 m length and 3 m mutual distance will be used as shown in Fig. 4.

The second example is to demonstrate a much more complicated and complex situation under clear sky conditions. Therefore the standard CIE Clear Sky, type 12 was chosen for a real location and time, i.e. at 8:30 a.m. on May 10th in Bratislava, Slovakia. For Bratislava geographical latitude 47.17°N and longitude 17.08°E is the solar altitude $\gamma_S = 40°$ and azimuth $\alpha_S = 110°$ on this day and hour. The typical luminous turbidity factor $T_v = 4$ and $D_v/E_v = 0.23$ were used for the urban environment in Bratislava. Thus the sky luminance pattern in Fig. 5A was found applying these parameters in the ModelSky program (Kocifaj and Darula, 2002) and the exterior diffuse illuminance $D_v = 63.7$ klx was calculated. It is to be noted that this program is applying a special orientation of the sky patterns with the sun-meridian on a horizontal line therefore the true North is inserted in Fig. 5A.

Due to the fact that sun-beams are striking some upper parts of the tube these are interreflected differently within tubes of various lengths. Therefore calculations had to be repeated for all chosen tubular guides documented in Fig. 5A–I. Note that the shortest 0.5 m light-tube redistributed the sky pattern and sun-beams on the diffuser as represented in Fig. 5B with the illuminance distribution on the working plane in Fig. 5C. In comparison with the usually used flux methods the HOLIGILM allows to predetermine

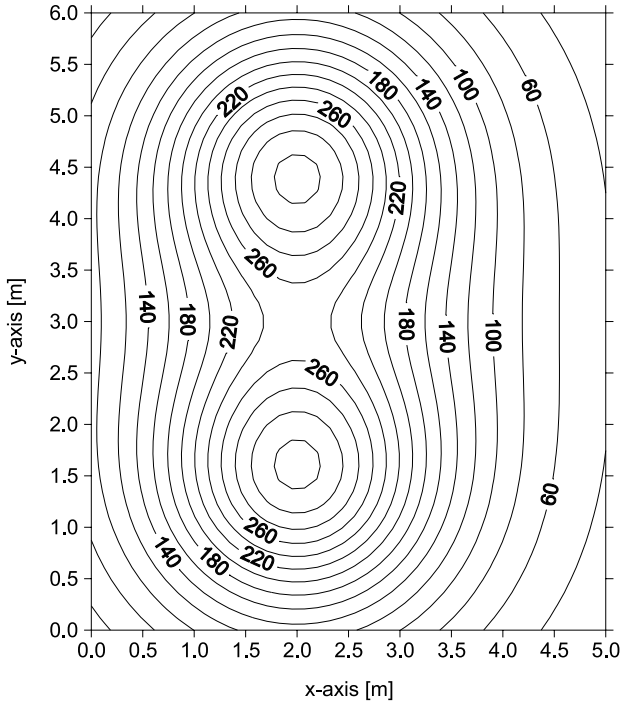

Fig. 6. Example of interior illuminance distribution with two 4.8 m tubes under CIE Clear Sky.

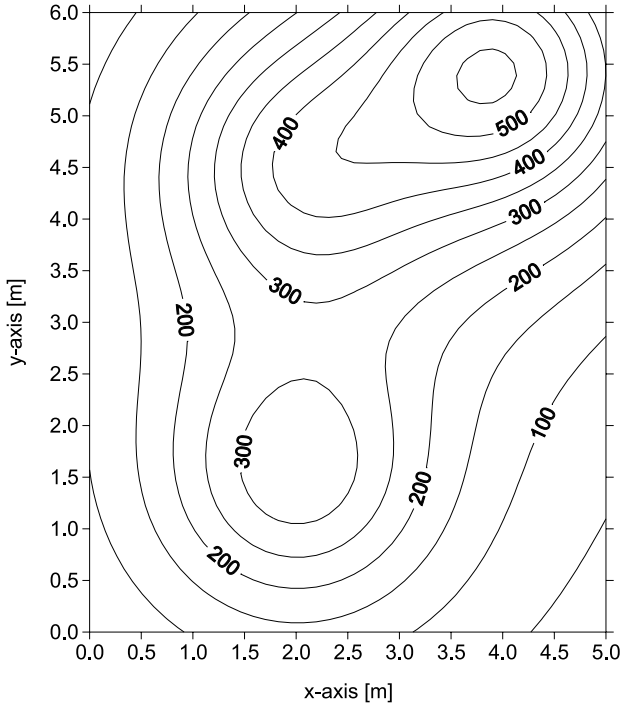

Fig. 7. Example of interior illuminance distribution with two 4.8 m and additional one 2.0 m tubes under CIE Clear Sky.

the different redistribution of sky patterns and solar beam due to multiple interreflections in shorter or longer hollow light guides. Thus while in the 0.5 m tube the sun image was turned to 180° (i.e. opposite sun-meridian side), in a 1 m tube the pattern on the diffuser is just on the sun-meridian side, i.e. the sun image is at 0° (Fig. 5D). The longer is the tube the sun image is directed more to the centre of the diffuser as represented in Fig. 5F and H. These sun images are creating the so called "hot-spots" as documented by photos of some diffusers, e.g. in Swift et al. (2006).

At the same time the diffusing properties of the diffuser in all cases result in the concentrated pattern of the illuminance distribution on the interior working plane with the decreasing lux levels in Fig. 5C, E, G and I, respectively. Also the effect of several light-tubes can be calculated by the HOLIGILM, as shown for two 4.8 m long tubes in Fig. 6 when the tubes are in a row in a 3 m distance or in a side way asymmetrical array of three tubes as in Fig. 7 under the same clear sky conditions. In comparison to overcast conditions under clear skies all interior illuminance levels are relatively higher especially when two or three light guides are applied.

6. Conclusions

Probably the most frequent hollow light guides are cylindrical tubes with high internal reflectance, a hemispherical cupola on top and a diffuser at their bottom. The illuminating engineering qualities of these vertical tubes are based on several advantages of the effective utilisation of daylight, namely:

- on the collection of skylight from those sky patches that have the highest luminance, i.e. from near zenith solid angles of the overcast and cloudy skies as well as the high luminance of solar corona sky parts on clear or turbid skies,
- on the possibility of "trapping" sunlight into the hollow guide under any sun position,
- on the mirror reflectance of the inner tube surface which is directing the light flow toward the diffuser placed on the ceiling of a sometimes windowless interior.

The calculation tool called HOLIGILM follows the classical and analytical approach of integrating sky and sun luminances within their solid propagation angles using the idea of ray-tracing. Respecting typical sky patterns standardised by either CIE or ISO as well as sun luminance or parallel sun beam illuminance under actual sun position and atmospheric turbidity, the HOLIGILM allows to predetermine interior illuminance distributions close to reality.

This paper describes the basic concept, formulae and examples with some results obtained by HOLIGILM valid for vertical cylindrical hollow light guides. The advantage of this method is also in the possibility to identify so called hot-spots on the tube diffuser, their redirection due to diffuser properties as well as the determination of interior illuminance on the working plane in absolute lux values.

The HOLIGILM will enable also different tests of tube adjustments or changes in their profiles, lengths and qual-

ities of their surface reflectance, covering domes or diffusers taking into account different sky luminance patterns and sun positions under various atmospheric conditions. Furthermore, this method will certainly be a useful tool to evaluate the effectiveness of particular hollow light guides in their year-round performance as well as their energy-efficient utilisation of sunlight and skylight in different climatic regions and under real local conditions.

Acknowledgements

This work was supported by the Grants SK-CZ-11006 and VEGA 2/5093/5.

References

Bracale, G., Mingozzi, A., Bottiglioni, S., 2001. Performance and daylighting applications of the tubularskylight. In: Proc. Conf. Lux Europa 2001, Reykjavik, pp. 360–384.

Carter, D.J., 2002. The measured and predicted performance of passive solar light pope system. Light. Res. Technol. 34 (1), 39–52.

Commission Internationale de l'Eclairage (CIE), 2003. Spatial distribution of daylight – CIE Standard General Sky. CIE Standard CIE S011/E: 2003. Bureau Central CIE, Vienna.

Commission Internationale de l'Éclairage (CIE), 2005. Tubular daylight guidance systems. Final Rep., TC 3-38. Bureau Central CIE, Vienna.

Darula, S., Kittler, R., 2002. Parametric definition of the daylight climate. Renew. Energy 26, 177–187.

Darula, S., Kittler, R., 2006. Twin system: descriptors for the evaluation of illuminance and irradiance availability. Build. Res. J. 54, 189–197.

Darula, S., Kittler, R., Gueymard, Ch.A., 2005. Reference luminous solar constant and solar luminance for illuminance calculations. Solar Energy 79, 559–565.

Darula, S., Kittler, R., Wittkopf, S., 2006. Outdoor illuminance levels in the tropics and their representation in the Virtual Sky Dome. Archit. Sci. Rev. 49, 301–313.

Fraas, L.M., Pyle, W.R., Ryason, P.R., 1983. Concentrated and piped sunlight for indoor illumination. Appl. Opt. 22, 578–582.

Gupta, A., Lee, J., Koshel, R.J., 2001. Design of efficient light pipes for illumination by an analytical approach. Appl. Opt. 40, 3640–3648.

Harrison, S.J., McCurdy, G.G., Cooke, R., 1998. Preliminary evaluation of the daylighting and thermal performance of cylindrical skylights. In: Proc. Conf. Daylighting, Ottawa, pp. 205–212.

International Standardisation Organisation (ISO), 2004. Spatial distribution of daylight: CIE Standard General Sky, ISO Standard 15469:2004.

Iqbal, M., 1983. An Introduction to Solar Radiation. Academic Press, Toronto.

Jenkins, D., Muneer, T., Kubie, J., 2005. A design tool for predicting the performances of light pipes. Energy Build. 37, 485–492.

Kittler, R., Darula, S., Perez, R., 1998. A Set of Standard Skies. Polygrafia Publ., Bratislava, Slovakia.

Kocifaj, M., Darula, S., 2002. ModelSky – jednoduchý nástroj pre modelovanie rozloženia jasu na oblohe (ModelSky – a simple tool for modelling the luminance distribution on the sky). Meteorologické zprávy 55 (4), 110–118.

Kocifaj, M., Lukáč, J., 1998. Using the multiple scattering theory for calculation of the radiation fluxes from experimental aerosol data. J. Quant. Spectrosc. Radiat. Transfer 60, 933–942.

Laouadi, A., 2004. Design with SkyVision: a computer tool to predict daylighting performance of skylights. NRCC-46752, Ontario, May 2–7, 2004, pp. 1–11.

Maradudin, A.A., Leskova, T.A., Méndez, E.R., 2003. Two-dimensional random surfaces that acts as circular diffusers. Opt. Lett. 28, 72–74.

Minin, I.N., 1988. Theory of Radiative Transfer in Planetary Atmospheres. Nauka (in Russian).

Oakley, G., Riffat, S.B., Shao, L., 2000. Daylight performance of light pipes. Solar Energy 69, 89–98.

Plch, J., Mohelnikova, J., 2005a. Tubular light guides in buildings. In: Proc. Conf. Solaris 2005, Athens, pp. 98–103.

Plch, J., Mohelnikova, J., 2005b. Light guides – daylight and energy saving system. In: Proc. Conf. Lus Europa 2005, Berlin, pp. 259–261.

Rosemann, A., Kaase, H., 2005. Lightpipe applications for daylighting systems. Solar Energy 78, 772–780.

Shao, L., Riffat, S.B., Hicks, W., Yohannes, I., 1997. A study of performance of light pipes under cloudy and sunny conditions in the UK. In: Proc. Conf. Right Light, 4, pp. 155–159.

Swift, P.D., Smith, G.B., 1995. Cylindrical mirror light pipes. Solar Energy Mater. Solar Cells 36, 159–168.

Swift, P.D., Smith, G.B., Franklin, J., 2006. Hotspots in cylindrical mirror light pipes: description and removal. Light. Res. Technol. 38, 19–31.

Zhang, X., Muneer, T., 2000. A mathematical model for the performance of light-pipes. Light. Res. Technol. 32, 141–146.

Zhang, X., Muneer, T., Kubie, J., 2002. A design guide for performance assessment of solar light-pipes. Light. Res. Technol. 34, 149–169.